Theor Appl Genet (2014) 127:2159–2171
DOI 10.1007/s00122-014-2369-9

ORIGINAL PAPER

Construction of a dense SNP map of a highly heterozygous diploid potato population and QTL analysis of tuber shape and eye depth

Ankush Prashar · Csaba Hornyik · Vanessa Young · Karen McLean · Sanjeev Kumar Sharma · M. Finlay B. Dale · Glenn J. Bryan

Received: 23 January 2014 / Accepted: 25 July 2014 / Published online: 27 August 2014

Abstract

Key message **Generation of a dense SNP-based linkage map of a diploid potato population and identification of major QTLs for tuber shape and eye depth on chromosomes 2 and 10.**

Abstract This paper reports the construction of a genetic map of a highly heterozygous full-sib diploid potato population (06H1) based on the use of a set of 8,303 single nucleotide polymorphism (SNP) markers. The map contains 1,355 distinct loci and 2,157 SNPs, 802 of which co-segregate with other markers. We find high levels of collinearity between the 12 chromosomal maps with a recently improved version of the potato genome assembly, with the expected genetic clustering in centromeric regions. The linkage maps are used in combination with highly detailed phenotypic assessments conducted over two growing seasons to perform quantitative trait loci analysis of two important potato traits, tuber shape and eye depth. The major loci segregating for tuber shape in 06H1 map to loci on chromosomes 2 and 10, with smaller effects mapping to three other chromosomes. A major locus for tuber eye depth co-locates with the tuber shape locus on chromosome 10. To assess when tuber shape is established in the developing tuber, we have performed staged observations of tuber formation. Our observations suggest that tuber shape is determined very early in tuber development.

Communicated by Herman J. van Eck.

Electronic supplementary material The online version of this article (doi:10.1007/s00122-014-2369-9) contains supplementary material, which is available to authorized users.

A. Prashar · C. Hornyik · K. McLean · S. K. Sharma · M. F. B. Dale · G. J. Bryan (✉)
The James Hutton Institute, Invergowrie, Dundee DD2 5DA, UK
e-mail: glenn.bryan@hutton.ac.uk

V. Young · M. F. B. Dale
Mylnefield Research Services, Invergowrie, Dundee DD2 5DA, UK

Introduction

Potato is the world's most important non-cereal food crop and consumed daily by more than a billion people (FAO). Cultivated potato is a highly heterozygous outbreeding crop which exhibits tetrasomic inheritance, these factors compromising genetic analysis and breeding. Despite these challenges, progress has been made in developing tools for linkage mapping and quantitative trait locus (QTL) analysis in tetraploid potato (Luo et al. 2001; Hackett et al. 2013). Most genetic analysis in potato has been performed using crosses between heterozygous diploid parents, and many diploid maps have been constructed for potato using a range of molecular marker types (e.g. Bonierbale et al. 1988; Bryan et al. 2002; Van Os et al. 2006). Potato linkage maps have been used for genetic analysis of many complex tuber traits (Van Eck 2007). Nonetheless, complex trait analysis in potato remains a challenging activity, and it is not straightforward to identify candidate genes directly from QTL mapping studies, unless other information (e.g. from transcriptomic or metabolomic studies) is available. With the publication of the potato genome (Potato Genome Sequencing Consortium 2011), it should now be possible to use linkage and QTL maps, given sufficient map density and resolution, to move towards more direct use of candidate gene approaches for trait gene identification. For example, the gene underlying the much studied and

highly important maturity trait of potato has recently been identified using this type of approach (Kloosterman et al. 2013).

Of the many potato tuber traits important to breeders, tuber shape and eye depth are of particular importance, both for fresh market uses and to the potato processing industry. Poor or irregular shape and deep eyes contribute to higher costs for the processing industry due to significant peeling losses. Consumers are not inclined to buy varieties showing deep eye depth, which makes peeling difficult. Thus, as these traits influence consumer consumption and trends in marketable value, breeding for shape uniformity and shallow eyes is highly important. Despite this, there are relatively few published genetical studies of these traits. The first detailed genetic study of tuber shape detected multiple alleles at a major locus on chromosome 10, whereby 'Round' alleles from both parents appeared to be dominant over alleles conferring long tuber shape (van Eck et al. 1994). Sliwka et al. (2008) studied the inheritance of several traits within a diploid hybrid population derived from several species and identified major QTLs accounting for between 6 and 15 % of the observed variance for tuber eye depth (chromosome 10), flesh colour (chromosome 4), shape (chromosome 2) and shape regularity (chromosome 3). They also identified minor QTLs associated with these traits, which challenges previous theories suggesting more or less qualitative control for eye depth (Maris 1966) and tuber shape (van Eck et al. 1994). Li et al. (2005) also identified a QTL for tuber eye depth on chromosome 10 and found it to be very closely linked to a major tuber shape QTL and also inferred monogenic control.

Recently, Felcher et al. (2012) have reported the construction of two diploid maps based on a newly developed single nucleotide polymorphism (SNP)-based platform, known as the Infinium 8303 Potato Array, the development of which was based on transcriptome sequencing from tetraploid potato cultivars (Hamilton et al. 2011). Felcher et al. (2012) integrated their maps with the published potato genome sequence (Potato Genome Sequencing Consortium 2011), allowing comparisons of collinearity between the maps with the genome assembly, a newer improved version of which has recently been published (Sharma et al. 2013). In this paper, we use the same SNP platform to construct a linkage map of a highly heterozygous 'Phureja-Tuberosum' hybrid diploid potato population (06H1); constructed by intercrossing two different clones resulting from Phureja x Tuberosum crosses. Moreover, we also compare our SNP map with the most recent version of the potato genome assembly (Sharma et al. 2013). QTL analysis of two of many traits segregating in this cross, namely tuber shape and eye depth, reveals similarities with previous work on these traits, and has also identified additional trait loci interacting with major-effect QTLs. Our findings will assist in the map-based isolation of genes determining tuber shape and eye depth in potato and should also prove useful for marker-assisted breeding. These results show the utility of both the newly developed SNP platform and the potato genome in the genetic dissection of potato traits.

Materials and methods

Plant material and field trialling

The mapping population used here (06H1) is a full-sibling progeny [$n = 186$ of a cross between two highly heterozygous diploid potato clones (HB171(13) and 99FT1b5)], both of which result from crosses between diploids of *Solanum tuberosum* group *Tuberosum* and *Solanum tuberosum* group *Phureja*. The HB171(13) clone was the blight-resistant parent of a cross reported by Bradshaw et al. (2006). The 99FT1b5 parent was used in a cross (FT.4) developed for the analysis of potato organoleptic traits and texture (G. Bryan, unpublished data).

Field trials were carried out as five plant plots per genotype replicated twice using alpha designs between 2009 and 2011 at Balruderry Farm, near Invergowrie, Dundee. Trialling of 186 clones and the two parents was performed as one block and seed tubers were planted in the last week of April, 30 cm apart in pre-made drills with 2 m distance between plots. All field trials went through standard agronomic practices for fertilizer and pesticide applications.

Phenotyping for tuber shape and eye depth

Tubers were harvested after physiological maturity and phenotyping was carried out for tuber shape and eye depth. Assessment for eye depth (5 tubers per plot) was based on a visual phenotypic scale of increasing 'commercial desirability' using a 1–9 scale, where 1 = very deep eyes and 9 = very shallow eyes. Evaluation for tuber shape was carried out using two approaches. In 2009 and 2010, tuber shape was visually assessed from the total produce of individual plots (5 tubers per plot) on a 1–4 'breeders scale', where 1–4 were represented as round (1), oval (2), long oval (3) and very long oval (4). A more analytical approach was used in 2010 and 2011 whereby tuber shape was evaluated quantitatively using length/width (LW) ratio as the numerical measure for the phenotypic value of tuber shape. Six tubers randomly selected from each plot in 2010 and 6–9 tubers per plot in 2011 shape were assessed using digital callipers (Mitutoyo UK Ltd.) by measuring the length and width of the tuber, a similar evaluation method as that described by Van Eck et al. (1994). For quantification, the distance between the rose (apex) and the heel (attachment of stolon) was defined as the length (length) and the

transversal axis perpendicular to the longitudinal axis was defined as the width (width). To compensate for some of the irregularities in tuber shape, the width of the tuber was measured on two perpendicular width axes, and the average of these measurements is regarded as the width value for each clone [i.e. width = 0.5 × (width1 + width2)]. The tubers with LW ratio higher than ~1.5 are referred to as 'elongated', whereas if the LW ratio was close to 1 they are classified as 'round'.

DNA extractions

Leaf material was collected from glasshouse grown plants of the 06H1 population and DNA was extracted from frozen 100 mg of leaf material using a Qiagen DNeasy plant mini kit (Qiagen)and quantified using a Nanodrop 1000 spectrophotometer (Thermo Scientific).

Genotyping

Hamilton et al. (2011) identified 69,011 SNPs using Illumina sequence data from commercially important processing cultivars Premier Russet, Atlantic and Snowden as well as pre-existing Sanger sequencing data from cultivars Bintje, Kennebec and Shepody. A core set of 8,303 SNPs have been used to design the "Infinium 8303 Potato Array", which covers 650 Mb of the potato genome (Felcher et al. 2012). Of the 8,303 SNPs, 3,018 (36.3 %) are targeted to candidate genes of interest, 536 (6.4 %) to pre-existing potato genetic markers and 4,749 (57.2 %) are designed to provide maximal genome coverage. DNA from the 06H1 population and parental clones (~50 ng/µl) was genotyped on an Illumina iScan Reader at Genprobe, Livingstone, UK utilising the Infinium HD Assay Ultra (Illumina, Inc., San Diego, CA) and the Infinium 8303 Potato Array. Results were analysed with the Illumina GenomeStudio software (Illumina, San Diego, CA). All polymorphic SNPs that segregated in either an approximate 1:1 or 1:2:1 ratio were selected for further analysis. All genotype calls were manually checked for accuracy and ambiguous data points that failed to cluster were scored as missing data.

Linkage map construction

Before constructing genetic maps, SNPs were filtered by excluding SNPs that were monomorphic (both parents homozygous) or that had poor quality data. SNP markers with missing parental genotype information and also SNPs where parental genotypes were inconsistent with progeny genotypic ratios were removed from map construction. Low quality SNPs also included those with NormR results <0.2 and SNPs with large numbers of missing values (20 % or more). Markers showing identical segregation patterns were excluded, with one marker per co-segregating group retained. A genetic map was constructed using regression mapping in JoinMap4.1 (Van Ooijen, 2006) using the 'cross-pollinated' population type (where <lmxll> was used when HB171(13) was heterozygous, <nnxnp> where 99FT1b5 was heterozygous and <hkxhk> where both parents were heterozygous). During the mapping process, markers with very high segregation distortion and with poor 'nearest neighbour fits' were excluded. The marker grouping process used a maximum LOD of 30.0 and the 12 linkage groups were created using the Kosambi mapping function.

QTL mapping

QTL mapping was performed with the computer programs MapQTL®6.0 (Van Ooijen 2009) and Genstat 15.1 (VSN International Ltd.). The non-parametric Kruskal–Wallis (KW) test supported in MapQTL version 6.0 was performed. In this method, a single marker analysis was used to test the association of a marker with the trait at significance $P \leq 0.001$. The identified QTL regions were further explored using single trait single environment QTL analysis using Genstat 15.1 where assessment for 2010 and 2011 data was carried out separately. This was done using composite interval mapping (CIM) controlling the effects of chromosomes onto the QTL being tested and so increasing the precision of QTL detection (Zeng 1994).

To identify interactions between different markers/QTL regions, interaction models were fitted with Genstat 15.1 using regression between different markers identified under the QTL regions during analysis.

Map comparison with potato genome

Revised physical positions for all the Illumina Potato 8303 Infinium array SNPs, reported by Felcher et al. (2012) using their customised version (2.1.11) of potato reference pseudomolecules (PMs), were obtained for the latest version (4.03) of PMs (Sharma et al. 2013). Unanchored SNPs (in the PMs) and SNPs showing discrepancy with respect to the chromosome assignments were not included in the genetic/physical map analysis (see Supplementary Table 1 for a list of these markers). Genome-wide recombination rates were estimated by comparing 06H1 linkage maps to the PM version 4.03. The local recombination rates for all the SNPs included in the genetic and physical maps comparison were calculated by locally adjusting a polynomial curve to the plot of genetic versus physical distances. The plots were generated using the MareyMap package which is an R-based tool that employs Tcl/Tk to build the graphical interface (Rezvoy et al. 2007). For each plot, the slope of the curve was fitted using the in-built 'lowess' (lowess

Table 1 SNP loci and marker numbers, map densities, and map lengths for each linkage group of 06H1 population

LG	No. SNPs	No. loci	No. of segregating loci					Genetic map length (cM)	Physical map length (Mb)	No. loci (SNPs) per cM	No. loci (SNPs) per Mb
			Maternal (lm × ll)		Paternal (nn × np)		Biparental (hk × hk)				
			Phase {0-}	Phase {1-}	Phase {-0}	Phase {-1}	–				
1	271	170	50	16	9	41	54	85.4	88.7	2.0 (3.2)	1.9 (3.1)
2	201	119	34	7	31	10	37	52.9	48.6	2.2 (3.8)	2.4 (4.1)
3	212	120	26	18	30	14	32	66.9	62.3	1.8 (3.2)	1.9 (3.4)
4	218	151	41	23	10	29	48	69.2	72.2	2.2 (3.1)	2.1 (3.0)
5	110	77	9	20	15	4	29	58.4	52.1	1.3 (1.9)	1.5 (2.1)
6	187	91	18	7	16	19	31	55.6	59.5	1.6 (3.4)	1.5 (3.1)
7	260	157	20	39	12	23	63	64.3	56.8	2.4 (4.0)	2.8 (4.6)
8	183	111	30	4	44	8	25	53.4	56.9	2.1 (3.4)	1.9 (3.2)
9	167	115	15	40	23	7	30	67.5	61.5	1.7 (2.5)	1.9 (2.7)
10	116	78	5	26	16	7	24	57.0	59.8	1.4 (2.0)	1.3 (1.9)
11	145	106	11	16	13	38	28	59.8	45.5	1.8 (2.4)	2.3 (3.2)
12	87	60	18	10	16	8	8	63.4	61.2	0.9 (1.4)	1.0 (1.4)
Total	2,157	1,355	277	226	235	208	409	753.99	725.0	1.8 (2.9)	1.9 (3.0)

for Locally WEighted Scatterplot Smoothing) interpolation method in the aforementioned R package.

Statistical analysis

Preliminary analysis of the phenotypic data was performed using Agrobase Generation II SQL (Agronomix Inc., MB Canada). Using Agrobase, phenotypic data were analysed using either an alpha analysis or randomised complete block (RCB) analysis. An alpha design is a balanced form of randomised complete block design which is aimed at detecting trends across trials through the use of sub-blocks. The RCB analysis was used if there was any missing data for a trait in both replicates, which precludes the alpha analysis. Agrobase was used to generate statistics for clone means, trait means and coefficients of variation. Clone means were used to plot trait distributions and for QTL analysis. All subsequent statistical analyses were carried out in Genstat 15.1.

Results

Linkage map construction

A total of 8,303 SNPs were used to screen the 06H1 population and 2,768 SNPs were polymorphic and used to create genetic maps. The markers excluded as a result of filtering processes comprise 1,380 with no or inconsistent parental scores, 4,059 as monomorphic and 96 with more than ~20 % missing data. The expected Mendelian segregation ratio of each marker in the mapping population was tested by the Chi square test ($P < 0.001$). Linkage analysis was performed using the remaining 2,768 markers and some markers showing highly significantly distorted segregation ratios and high 'nearest neighbour fits' were removed from individual maps. Consequently, the remaining 2,157 markers, which include markers co-segregating with at least one other marker were used to create the 12 linkage group maps comprising 1,355 unique loci (Supplementary Fig. 1). These maps provide dense coverage of the potato genome, with an average one marker per 330 kb across the entire genome assembly and 1 cM corresponding to ~960 kb. The total map length was ~754 cM with chromosome 1 being the longest (~85 cM) and chromosome 2 (~53 cM) as the shortest of the genetic maps (Table 1).

Comparisons of linkage maps with potato genome assembly

Markers on the 12 06H1 linkage maps were compared with their positions on the potato PMs v4.03 (Sharma et al. 2013) to assess the quality of our maps as well as the degree of correspondence between them and the revised potato genome assembly (Fig. 1; Supplementary Fig. 2). A further goal of the study was to examine the frequency and distribution of recombination in defined regions along the 12 potato chromosomes. The clearly superior alignments of our 06H1 genetic maps (Fig. 1a, b; Supplementary Fig. 2a, b) as well as those published by Felcher et al. (2012) (Fig. 1c, d) with the more recently released versions of the potato genome PMs (Sharma et al. 2013), as compared with those (v2.11)

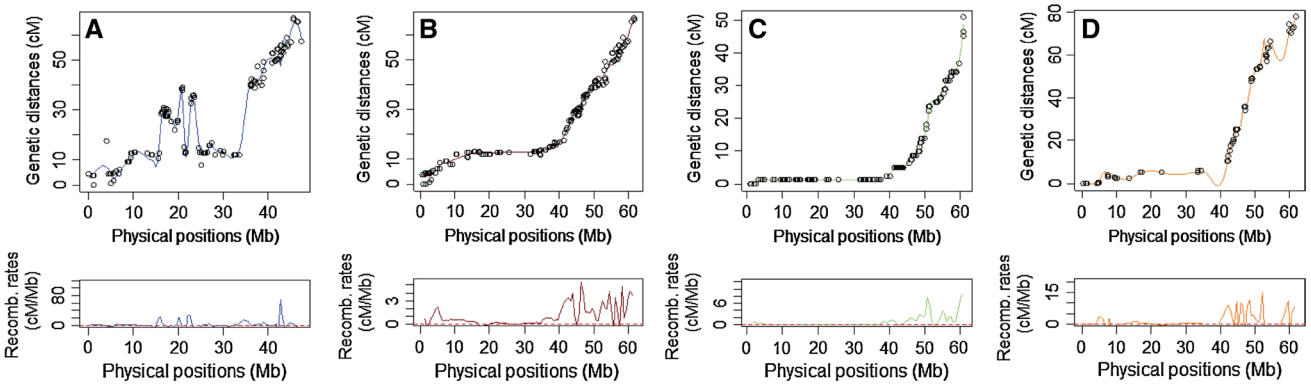

Fig. 1 Graphical representation showing the relationship between genetic map and physical map for chromosome 3 and the estimated recombinations. **a** Comparison of 06H1 chromosome 3 linkage map with DM genome physical map v2.1.11 (used by Felcher et al. 2012). **b** Comparison of 06H1 chromosome 3 linkage map with DM genome physical map v4.03 (latest version in Sharma et al. 2013). **c** Comparison of Chromosome 3 genetic map of diploid population (D84) used by Felcher et al. (2012) with DM genome physical map v4.03 to demonstrate the improvement in new pseudomolecule version. **d** Comparison of Chromosome 3 genetic map of diploid population (*DRH*) used by Felcher et al. (2012) with DM genome physical map v4.03 to demonstrate the improvement in new pseudomolecule version

previously used for comparisons by Felcher et al. (2012) demonstrate the improved quality of the latest release. The 06H1 linkage maps generally exhibit very good collinearity with the genome, and our data correlate well with what is known about potato chromosome structure. For most of the 12 chromosomes, the typical plot of genetic vs physical distance is observed with markedly reduced recombination in pericentromeric regions, and varying recombination rates in euchromatic regions. These types of plot were useful during linkage map construction, regions of reduced collinearity being used to re-examine both mapping and assembly data. In some cases, these incongruities resulted from use of the Illumina software for automated calling of genotypic scores, and in several cases by manually calling a marker it was possible to improve the linkage maps as well as the correspondence between maps and genome assembly. The maps reported by Felcher et al. (2012) contain maps based on segregation from only one heterozygous parent, whereas the 06H1 maps reported here are based on two heterozygous parental clones. This factor may help explain why the 'genome comparison' plots using the previously published 'uniparental' maps shown in Fig. 1c, d are 'smoother' and more linear in centromeric regions than our maps (Fig. 1a, b), which appear to show some recombination in these regions. This observation could be an artefact of making maps based on four parental haplotype phases and could also reflect differences in recombination rates between the parents of the 06H1 cross.

Tuber shape analysis

Tuber shape was assessed from field grown tubers of the 06H1 population in 2009 and 2010 using a 1–4 'breeder's scale' and in 2010 and 2011 using the more quantitative LW method described. LW ratios of individual tubers were calculated where the width is the average of the two width measurements (perpendicular to each other in both directions perpendicular to the longitudinal axis). The two scoring methods are highly correlated with a value of the correlation coefficient r, of 0.91 for the 2010 data, the only year both approaches were used and for which a direct comparison is possible. The high correlation between 'measured' (i.e. LW) and 'assessed' tuber shape suggests that rapid visual assessment method is a suitable tool for shape analysis in potato breeding programs, but the reproducibility and objectivity of measurement by calliper provide an important advantage for detailed genetical studies.

There were also strong correlations between the data collected over the 2 years of assessment using each method, $r = 0.81$ for 2009 vs 2010 for the qualitative '1–4' scoring method) and $r = 0.89$ for 2010 vs 2011 for the quantitative LW assessment. The correlations for tuber shape for within year replicates and also between years were highly significant and 'broad-sense' heritabilities were estimated at >0.90 for both methods suggesting that tuber shape is very largely controlled by genetic factors. All further analysis presented here is based on the more quantitative LW data. The overall range of clone LW values, averaged over 2 years, is from 0.77 to 2.58. Interestingly, the LW ratio does not only range from ~1 (i.e. round) to values greater than 2 (i.e. elongated), we also observe LW values less than 1 in 40 clones of the 06H1 progeny (Fig. 2). This effectively means that the distance between the rose and heel of the tuber is less than the average tuber width, giving these tubers a somewhat compressed appearance. According to the observed distribution of tuber measurements,

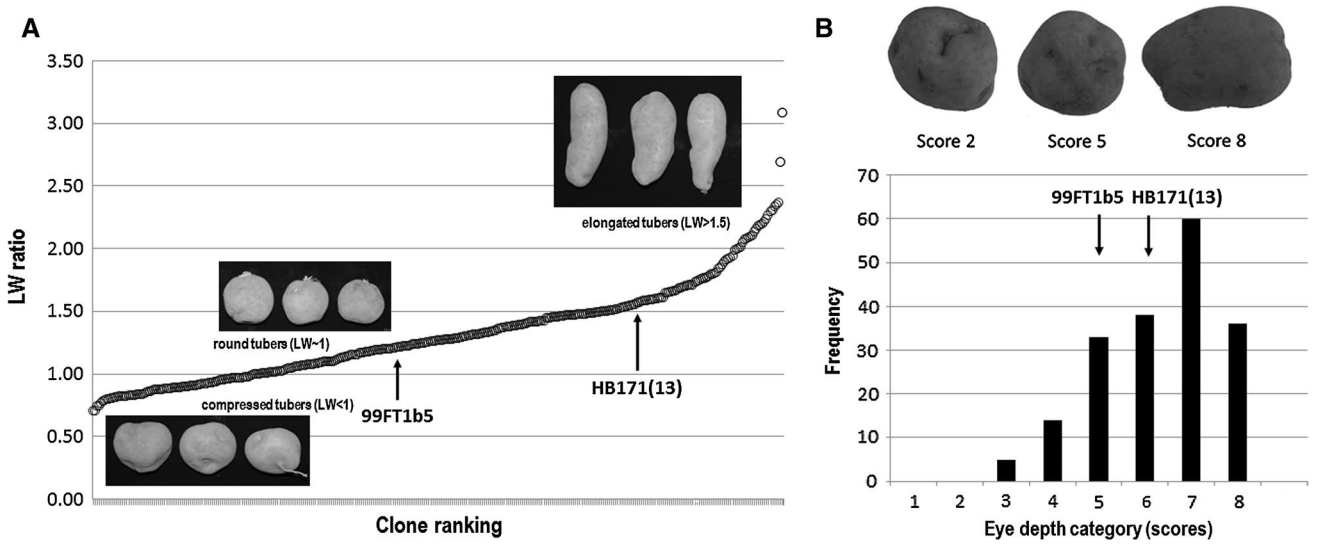

Fig. 2 **a** Graphical representation of the length width ratio range for tuber shape phenotypes in 06H1 population (mean ratio of 2010 and 2011) with corresponding images showing the defined classes of compressed tubers, round tubers and elongated tubers along the plot. **b** Illustration of tuber eye depth phenotypes over different eye depth scores and histogram displaying the frequency of different eye depth categories in scored in the population

we defined three basic categories for tuber shape, round, where the length and width are similar (LW ratio ~1); elongated, where length is larger than width (LW ratio >1.5), and 'compressed', these tubers showing shorter length than width (LW ratio <1). The rose and heel of these tubers are compressed into the tuber and they assume more of a "doughnut" shape (Fig. 2a). The average LW ratio for individual tubers of each clone and replicate was calculated for the two replicated trials in 2010 and 2011 and resulted in the LW ratio characteristic for the tuber shape of each clone in each year. The mean LW values across the 2 years are plotted graphically in Fig. 2a, ranked in order of increasing LW ratio. Three clones (06H1.a2, 06H1.a149, 06H1.a345) that produced curved tubers were identified in the population, with mean LW ratios of 2.58, 2.11 and 3.15. Such a low frequency of clones with curved tubers precludes further analysis of this trait.

Analysis of eye depth

Tuber eye depth was assessed on a 1–9 scale in 2009 and 2010 where 1 = very deep eyes and 9 = very shallow eyes (Fig. 2b). The trait was approximately normally distributed, with a truncated distribution at the 'shallow eye' end due to a lack of genotypes scoring '9', and with a mean value of 6.06 in both years. As seen with tuber shape, there was good agreement between replicates and broad-sense heritability was estimated at ~0.82. The correlation r between the clone means for the 2 years assessed was 0.79. Our data suggest that shape and eye depth are significantly correlated (~0.65 between eye depth 2010 vs LW 2010), such that longer tubers have a tendency to have more shallow eyes. In keeping with this the parent [HB171(13), mean eye depth = 6.7] with longer tubers has slightly shallower eyes than the rounder parent (99FT1b5, mean eye depth = 5.9) (Fig. 2).

QTL analysis of shape and eye depth in the 06H1 population

QTL analysis was performed using the 06H1 linkage map and the LW ratio tuber shape and eye depth data scored on a 1–9 scale of decreasing eye depth. Initially, data were subjected to non-parametric K–W analysis in MapQTL6. For tuber shape LW ratio, two groups of markers with significant K* values were detected on chromosomes 2 and 10. For chromosome 10, a set of paternal (nn × np) markers at about 40 cM showed the highest K* values, with marker c1_8020 showing the highest K* values 80.8 and 84.2 (both $P < 0.0001$) in 2010 and 2011, respectively. For chromosome 2, a set of maternal (lm × ll) markers at about 20 cM were most significantly associated with LW tuber shape scores. Of these marker c2_46885 showed the highest K* scores, 26.1 and 32.3 (both $P < 0.0001$) in 2010 and 2011, respectively. The mean and ranges of LWvalues for the four genotypic classes for these two groups of uniparental markers are, in increasing order of mean LW value: homozygote at LG2 and heterozygote at LG10 has mean LW = 0.98 (0.77–1.29), heterozygote both at LG2 and LG10 has mean LW = 1.31 (0.80–1.75), homozygote both at LG2 and LG10 has mean LW = 1.47 (1.03–1.96) and LG2 heterozygote, LG10 homozygote has mean LW = 1.85 (0.84–2.58).

Table 2 QTLs detected for shape and eye depth using composite interval mapping and the relative additive and dominance effect at the location

Year	LG	Locus	Position (cM)	$-\log_{10}(P)$	Add. Eff P1	SE	Add. Eff P2	SE	Dom. Eff	SE
Tuber shape										
2010	2	c1_5091	16.94	16.89	0.169	0.017	−0.036	0.017	−0.023	0.017
2010	9	c2_3066	57.51	5.35	−0.090	0.017	0.001	0.018	−0.008	0.018
2010	10	c1_8020	40.48	28.97	0.025	0.018	−0.236	0.017	−0.013	0.018
2011	1	c2_6839	7.32	4.90	0.005	0.017	−0.068	0.017	−0.058	0.017
2011	2	c2_51115	19.72	24.93	0.228	0.018	−0.010	0.018	−0.022	0.018
2011	3	c2_26454	50.57	7.55	−0.053	0.017	−0.098	0.018	−0.017	0.018
2011	10	c1_8020	40.48	36.88	0.008	0.019	−0.293	0.017	0.032	0.019
Eye depth										
2009	2	c2_7422	39.30	4.798	0.266	0.057	0.079	0.056	0.059	0.057
2009	3	c2_37119	66.93	4.741	−0.332	0.067	0.011	0.056	0.075	0.067
2009	10	c1_8020	40.48	26.022	0.156	0.061	−0.714	0.055	−0.005	0.061
2010	10	c1_8020	40.48	19.021	0.167	0.082	−0.794	0.075	0.029	0.082

The effects detected by Genstat in the table are half the value of the total effects for the cross-pollinated population (predicted from allele substitution). This is due to the fact that the "indicator values" used in Genstat range from −1 to +1 (giving the additive effects as −a and +a) instead of 0 to 1

From these data it is clear that, in keeping with previous studies, the locus on chromosome 10 exhibits a larger phenotypic effect on tuber shape than the chromosome 2 locus. The means over the 2 years for the two observed chromosome 10 genotypic classes (nn = 1.66, np = 1.14) differ by 0.52, while those for locus on LG2 (lm = 1.58, ll = 1.22) differ by 0.36. There is considerable phenotypic overlap between the four genotypic classes suggesting that a simple 'two locus' model of tuber shape is insufficient to wholly explain the observed pattern of variation in tuber shape in the 06H1 population, as measured by LW ratios. Simple interval mapping (SIM) in MapQTL6 yielded broadly similar results (data not shown).

A more sophisticated CIM approach was adopted using Genstat 15.1. A 'single environment single trait' approach was used, whereby each assessment year (2010 and 2011) was analysed separately. The routine DQSQTLSCAN (QSQTLSCAN procedure) was used and a genome-wide threshold of 0.01 was used to select QTL ($-\log_{10}$P value of 4.176 at 1 %). Initially, a SIM approach was used with a maximum step size of 20 cM and this identified the same QTL effects on chromosomes 2 and 10 as the K–W analysis and interval mapping analysis with MapQTL. SIM was followed by CIM, where QTLs detected by SIM were used as co-factors, extending the co-factor selection in subsequent iterations and which aimed to remove a co-factor from the model if another QTL was evaluated within 10 cM. Four (2010) and three (2011) rounds of CIM led to the detection of further QTL effects on chromosome 1 at ~7 cM (c2_6839) in 2011, chromosome 3 at ~51 cM (c2_26454) in 2011, and chromosome 9 at ~57 cM (c2_3066) in 2010. The QTL effects detected by the CIM analysis are summarised in Table 2 and shown graphically in Fig. 3a. The QTL analysis performed in Genstat uses indicator variables of −1 and +1 for the two genotypic classes which explains why the additive model parameters (Table 2) are roughly half the magnitude of the differences in phenotypic means for the two genotypes at each locus given in the previous paragraph. The largest effects are additive effects as detected by the previous K–W analysis, that is a maternally (P1) inherited effect increasing LW (0.169 in 2010, 0.228 in 2011) on chromosome 2, and a paternally (P2) inherited effect decreasing LW (−0.236 in 2010, −0.293 in 2011) on chromosome 10. However, there are also small additive effects detectable on chromosome 1, mainly a small paternally inherited negative effect on LW in 2011 (−0.068). Interestingly, there is a small but significant negative dominance effect at this locus in 2011 (−0.058). The negative QTL effect on chromosome 3 in 2011 appears to be inherited from both parents (−0.053 from maternal P1, −0.098 from paternal parent P2). The effect (−0.09) detected on chromosome 9 in 2010 originates from the maternal parent. Tests for interactions between these QTL effects showed that there were small but significant interactions between the chromosome 2 effect with the smaller chromosome 9 and 3 QTLs in 2010 and 2011, respectively (Table 3). The interaction model was fitted with parameters used from mapped QTLs. The most significant SNP underlying these QTLs was replaced by a neighbouring closely linked SNP depending upon the additive or dominance QTL effect at that chromosome location (more details are provided in Table 3).

K–W analysis of the eye depth data scored on a 1–9 scale revealed a large effect QTL at ~40.5 cM on

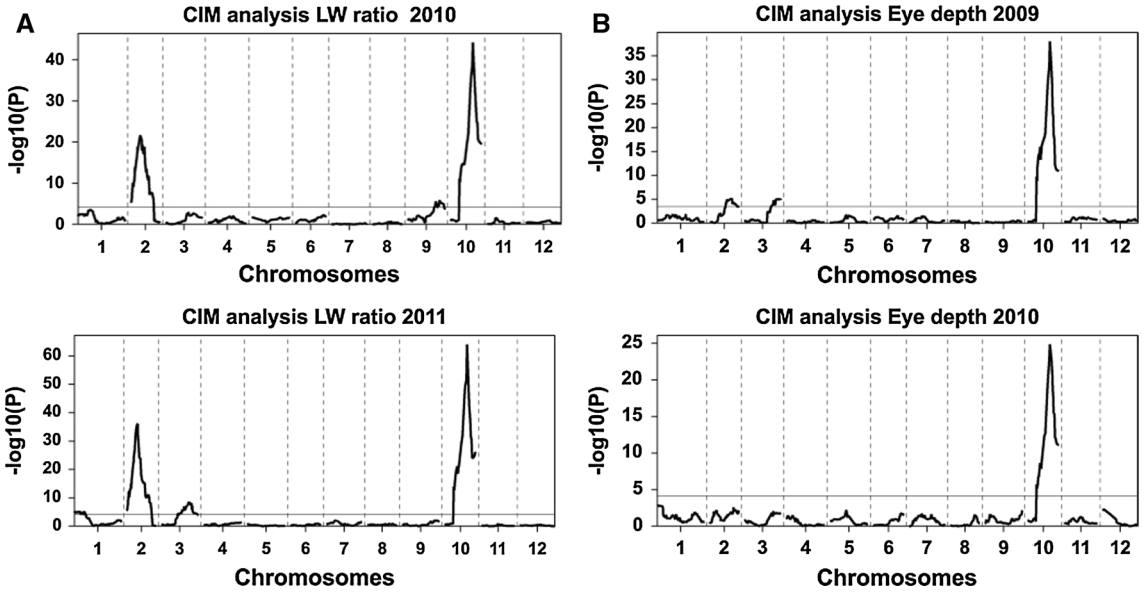

Fig. 3 QTL plots showing results of composite interval mapping for **a** Tuber shape as measured by LW ratio. **b** Eye depth. Upper panel shows 2010 data, lower panel 2011 data in both (**a**) and (**b**). Routine DQSQTLSCAN in Genstat using single trait single environment was used for analysis and a genome-wide threshold of 0.01 was used to select QTL ($-\log_{10}$P value of 4.176 at 1 %). Threshold represented by the solid horizontal line in the graphs

Table 3 Analysis of variance representing interaction model between significant QTL effects for tuber shape LW data in 2010 and 2011

Linkage group	Parameter		*df*	m.s.	v.r.	F pr.
	Most significant SNP underlying QTL effect	SNP used in interaction model based on QTL effect (additive1/additive 2/dominance)				
Interaction model 2010						
10	C1_8020	C1_8020	1	8.86	191.24	<0.001
2	C1_5091	C1_13923	1	4.12	88.81	<0.001
9	C2_3066	C2_43241	1	1.323	28.55	<0.001
2*9	C1_5091*C2_3066	C1_13923*C2_43241	1	0.62	13.32	<0.001
	Residual		173	0.05		
	Total		177	0.13		
Interaction model 2011						
2	C2_51115	C1_13923	1	6.65	107.5	<0.001
10	C1_8020	C1_8020	1	14.08	227.6	<0.001
1	C2_6839	C2_6839	2	0.30	4.92	0.008
3	C2_26454	C1_4576	2	0.15	2.4	0.094
2*3	C2_51115*C2_26454	C1_13923*C1_4576	2	0.29	4.68	0.01
	Residual		169	0.06		
	Total		177	0.18		

Parameter column has been divided into two columns (a) SNPs from QTL locations in Table 2 (C1_8020, C1_5091, C2_3066) (b) The significant SNPs replaced with linked SNPs at the nearest location, based on additive1, additive 2 and dominance effect of the significant SNPs underlying QTL. For e.g. C1_5091 on LG2 from Table 3 was replaced by C1_13923 as QTL had a maternal additive effect and C1_13923 is a maternal marker

chromosome 10, the largest effect being observed for paternal marker c1_8020 (K* values of 83.93 and 74.97 for 2009 and 2010, respectively, $P < 0.0001$). This QTL maps to the exact same map position as the large effect on tuber shape on LG10. CIM analysis (Table 2, Fig. 3b) shows the presence of this QTL, as well as two smaller QTLs for eye

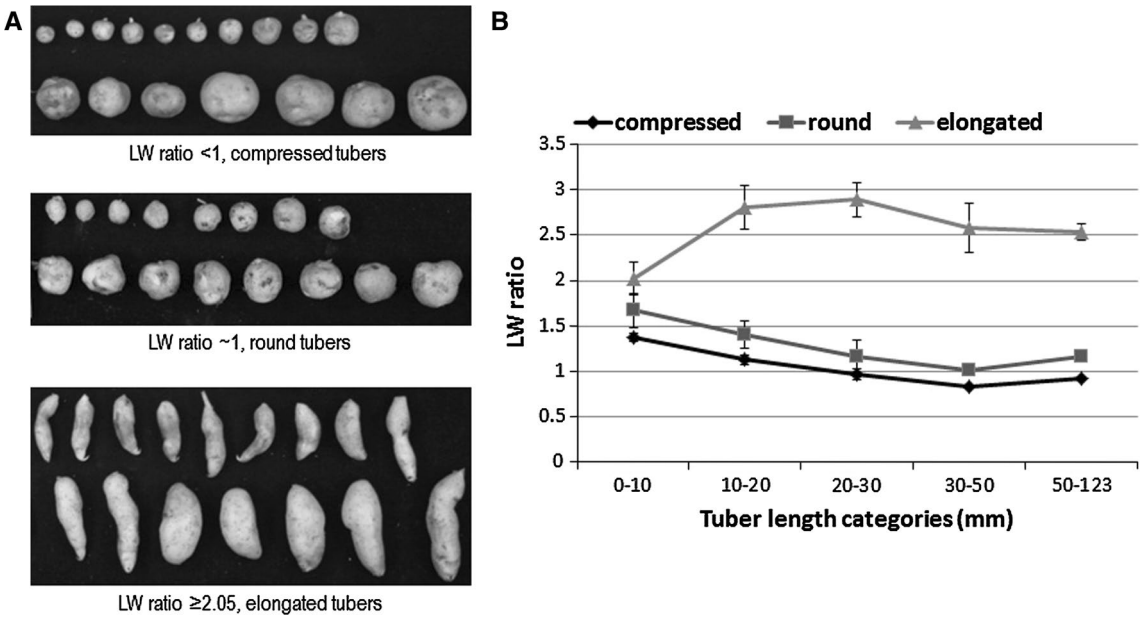

Fig. 4 Tuber shape response during tuber development. **a** Images of tubers of the three main defined shape categories showing the tuber shape at initiation and at full maturity. **b** Plots of LW for the three selected shape categories for different tuber length values

depth in 2009 on chromosomes 2 (c2_7422, 39.3 cM) and 3 (c2_37119, 66.93 cM). Only additive effects for these QTLs are significant, the largest effect overall being the paternal chromosome 10 allele acting to decrease the eye depth score, so causing a deeper eye phenotype.

Tuber shape is determined early during development

To assess how early during tuber development tuber shape is determined, we studied the shape of tubers from a 'tuber initiation' study performed during the 2011 growing season. Tuber 'initials' and small tubers up to the size of 123 mm were measured using the same calliper-based method as previously described. Ten clones of the 06H1 population for each of the three main tuber shape categories (long, round, compressed) were chosen to follow tuber development in replicated field trials which involved harvesting from the field at 5 different time points during the growing season (Fig. 4a). These three groups of tubers had average 2010 LW ratios of: elongated, mean LW = 2.25 (range 2.07–2.69); round, mean LW = 1.00 (range 0.97–1.01); compressed, mean LW = 0.81 (range 0.74–0.84). At each harvest, different sizes of tubers were measured because the clones in the population initiated tubers at different times, moreover, on the same plants we found tubers of different sizes due to tuber initiation starting at different times.

The tubers were categorised according to the following length categories: 0–10, 10–20, 20–30, 30–50 and 50–123 mm. LW ratio of tubers were determined and compared as was described previously (Fig. 4a, b). Box plot analysis of tuber length categories confirms the difference among the tuber shape categories (Supplementary Fig 3). Figure 4b shows that if the tubers were small (<10 mm), reliable detection of differences in the LW ratio can still be detected. Compressed tuber bearing clones showed the smallest LW ratio (1.4), round and elongated tuber bearing clones had similar, but higher LW ratio (1.5–2) compared to clones with compressed tubers. Interestingly, at this early stage of development, all the clones showed relatively high LW ratios, presumably reflecting the longitudinal axis on which tuber development initiates. Compressed and round tuber bearing clones had higher LW ratios at an early stage than later in development. For these groups of clones, we observed a decrease in LW ratio during tuber development, gradually getting closer to the ratio measured in fully developed tubers. There is a small but significant difference in mean LW between the compressed and round tubers throughout development, showing that the shape for these categories is well determined from an early time point of tuber initiation and development. Tubers originating from long tuber bearing clones always showed high LW ratio indicating that tuber shape for elongated tubers is also determined early during tuber formation.

Discussion

In this paper, we report the construction of a new SNP-based diploid genetic map of potato from a highly

heterozygous diploid potato cross segregating for many traits relevant to potato breeding activities. The potato SNP platform used here has been deployed in other potato studies (Felcher et al. 2012; Hackett et al. 2013) and is likely to be used in others subject to its continued availability, although re-sequencing based approaches for potato genotyping offer new possibilities (Uitdewilligen et al. 2013). The maps reported here show high levels of collinearity with the diploid and tetraploid maps previously reported using this SNP platform (data not shown). Construction of several linkage maps using this platform will allow high-quality alignments between linkage maps from different crosses. The vast majority of SNPs can be precisely and uniquely located in the potato genome, therefore genetic maps can be aligned directly to the latest potato genome PMs (Sharma et al. 2013). A consequence of this, as we demonstrate, is that observation of high levels of collinearity between maps and the genome provide mutual confirmation of the linkage mapping and genome assembly processes. Discordances, where observed, point towards either structural rearrangements or errors in genome assembly or mapping, as observed by Felcher et al. (2012), which can be further investigated and ultimately resolved in most cases. The maps presented here show a considerably higher degree of collinearity to the current potato genome PMs (v4.03) (Fig. 1, Supplementary Fig. 2) than to previous versions, highlighting the improvement in the potato genome assembly since its publication (Potato Genome Sequencing Consortium 2011; Sharma et al. 2013). The use of high density genetic maps has the potential to further improve this important genome resource. A further benefit of sequence based markers is that they permit the local genome sequence to be 'interrogated'. For example the genome sequence surrounding any locus of interest can be used to design further genetic markers, for example for the purposes of fine mapping a particular trait gene as a prelude to identifying candidate genes.

The map reported here contains 2,157 markers of which 802 are placed in bins due to their co-segregation with other mapped markers. The map genetically anchors ~477 Mb of the DM genome assembly, which is slightly more (21 %) than the 394 Mb anchored by the DMDD map used to anchor the DM genome (Sharma et al. 2013). The SNP markers on the platform used here were developed from a set of only six tetraploid potato cultivars (Atlantic, Premier Russet, Snowden, Bintje, Kennebec, Shepody). The diploid cross used here does not segregate for ~4,000 of the polymorphisms included in the SNP platform, and a tetraploid cross recently reported failed to segregate for about 2,200 of these SNPs (Hackett et al. 2013). This raises the question of whether it is necessary to define a larger more widely representative set of SNPs for potato mapping studies, and from which material these SNPs should be identified.

We have performed a detailed QTL analysis of two traits that segregate in the 06H1 cross, namely tuber shape and eye depth. Our results compare well with the few previous published studies of these traits, although it is difficult to perform detailed comparisons between maps as different types of markers are used, and some older maps do not have the resolution of the maps published here. Given these issues, it is highly likely that we have identified the same loci for tuber shape and eye depth as previously published by several authors (van Eck et al. 1994; Sliwka et al. 2008; Li et al. 2005).The locus on chromosome 10 for tuber shape and eye depth is almost certainly at the same position as that reported by Van Eck et al. (1994) for tuber shape and by Li et al. (2005) and Sliwka et al. (2008) for eye depth. However, in this study, unlike Li et al. (2005) there does not appear to be any separation of the loci for shape and eye depth, the same marker (c1_8020) showing the highest association with both traits. Our data are based on a highly detailed shape scoring method based on actual measurements, and a more detailed eye depth score (1–9), whereas these in Li et al. (2005) only use a 'three point' scoring system for each trait. Van Eck (2007) has discussed this issue, and suggests approaches that may be used to unravel the conundrum of whether tuber shape and eye depth are determined by the same gene or different genes that are very tightly linked. We observed only a single clone (06H1.a250) that seems to break the strong correlation between the two traits, showing a mean LW of ~1.75 and a mean eye depth of 4.75. This clone could potentially be used as a parent to generate a new population that may help in addressing this tantalising issue. In our view, it remains likely that a single gene is exerting a pleiotropic effect on the two highly correlated traits that cannot be separated genetically in this analysis.

The locus detected in this analysis on chromosome 2 is almost certainly at the same position as that reported by Sliwka et al. (2008). The marker most tightly linked to this QTL in the 06H1 cross is c2_46885, which maps to genome superscaffold PGSC0003DMB000000552. The markers most significantly associated with tuber shape in the diploid cross used by Sliwka et al. (2008) appear to be contained in potato genome superscaffolds PGSC0003DMB000000406 (GP86) and PGSC0003DMB000000141 (StPAD4 and Gp321), which are the two superscaffolds immediately adjacent to and 'north' of superscaffold PGSC0003DMB000000552 in the genome PMs (Sharma et al. 2013). Thus, a second major shape locus is defined in potato. We also report the detection of three smaller QTLs on chromosomes 1, 3 and 9 which are sometimes at the limit of detection, but which serve along with the larger effect loci to give a continuum of shape scores in the 06H1 progeny. We do not detect the small effect locus on chromosome 11 reported by Sliwka

Table 4 (a) Predicted LW ratio associated with the genotypes at the three interacting loci on LG2, LG9 and LG10 in 2010 data and (b) LG1, LG2 and LG10 in 2011

(a)

Trait	C2_43241 (LG9) = lm				C2_43241 (LG9) = ll			
	c1_8020 (LG10) = nn		C1_8020 (LG10) = np		c1_8020 (LG10) = nn		C1_8020 (LG10) = np	
	c1_13923 (LG2) = ll	c1_13923 (LG2) = lm	c1_13923 (LG2) = ll	c1_13923 (LG2) = lm	c1_13923 (LG2) = ll	c1_13923 (LG2) = lm	c1_13923 (LG2) = ll	c1_13923 (LG2) = lm
LW ratio_2010	1.383 (0.029)	1.598 (0.038)	0.906 (0.032)	1.122(0.039)	1.469 (0.037)	1.935 (0.046)	0.992 (0.03538)	1.458 (0.04442)

(b)

Trait	C2_6839 (LG1) = hh				C2_6839 (LG1) = hk				C2_6839 (LG1) = kk			
	C1_13923 (LG2) = lm		C1_13923 (LG2) = ll		C1_13923 (LG2) = lm		C1_13923 (LG2) = ll		C1_13923 (LG2) = lm		C1_13923 (LG2) = ll	
	C1_8020 (LG10) = nn	C1_8020 (LG10) = np	C1_8020 (LG10) = nn	C1_8020 (LG10) = np	C1_8020 (LG10) = nn	C1_8020 (LG10) = np	C1_8020 (LG10) = nn	C1_8020 (LG10) = np	C1_8020 (LG10) = nn	C1_8020 (LG10) = np	C1_8020 (LG10) = nn	C1_8020 (LG10) = np
LW ratio_2011	1.518 (0.044)	0.959 (0.045)	1.953 (0.047)	1.393 (0.047)	1.478 (0.036)	0.918 (0.036)	1.912 (0.041)	1.353 (0.041)	1.652 (0.044)	1.092 (0.046)	2.086 (0.052)	1.526 (0.052)

Standard errors are in brackets

et al. (2008). Interestingly, we see a shape class whereby the LW values are less than one, and which have a 'compressed' tuber phenotype. Further studies are required to demonstrate whether loci influencing tuber shape interact, and if so, the precise molecular and developmental mechanisms involved in generating this peculiar phenomenon.

The population used in this study (06H1) is interesting in that is a cross between two diploid 'Phureja-Tuberosum' hybrids, and as such may be expected to show marker haplotypes similar to the DM reference genome, which is based on sequencing of a Phureja doubled monoploid (Potato Genome Sequencing Consortium 2011). When the parental SNP marker haplotypes for chromosomes 2 and 10 are compared to their DM counterparts, it does appear that two haplotypes (phase 1 of both parents) of chromosome 2 are quite similar (~62 % identity) to the equivalent DM haplotype (data not shown). Interestingly, the data suggest that the 'long' alleles at the chromosome 2 locus originate from the phase 0 alleles from the maternal parent. This clone contains late blight resistance introgressed from *Solanum demissum*, so it is interesting to speculate that this species may represent the origin of the allele on chromosome 2 conferring longer shape (Bradshaw et al. 2006). For chromosome 10 the situation is less clear, with three haplotypes showing a strong similarity to DM (57–70 % identity). However, the alleles at the QTL locus on chromosome 10 are derived from the 'phase 0' haplotype of the male parent, which exhibits the lowest level of identity (~48 %) to the DM haplotype for this chromosome.

In the 06H1 cross loci on at least five chromosomes interact in some way to control tuber shape development. It is interesting to speculate that the dominance relationships may be different at the two major loci, rounder tubers being conferred by the heterozygous genotype at the major-effect locus on chromosome 10, with longer tubers being produced by heterozygotes at the chromosome 2 locus. It is problematic to make inferences regarding dominance at these loci, when the most tightly linked markers exhibit only two genotypic classes (i.e. one homozygote and heterozygote). Our QTL analysis provides little evidence for dominance effects, save a small negative effect on LW ratio on chromosome 2 in 2011. Further work is required to establish the true dominance relationships at these loci. This would entail generation of genotypes homozygous for the alleles only found in heterozygous condition in this cross or examination of data from tetraploid samples with LW and marker dosage data.

For further inspection of the QTL results, tests for interactions were carried out between different QTL positions and their linked markers (Graham et al. 2011). Where required, the markers showing the highest LOD score at the QTL location were substituted with closely linked significant markers based on the additive or dominance effects detected. As an example for 2010 data, there were three loci linked to the QTL regions (c1_5091 on chromosome 2, c2_3066 on chromosome 9 and c1_8020 on chromosome 10). Chromosome 2 and 9 showed the additive model based on parent 1 effects and chromosome 10 showed an additive effect from parent 2. Initially, a regression model was fitted by considering all these QTLs and their interactions. Model parameters which were non-significant in the first model were eliminated and new models were fitted. The 2010 data showed a significant interaction between loci on chromosome 2 and 9. A similar model fitting analysis was performed for 2011 data, which detected a significant interaction between the loci on chromosomes 2 and 3. The analysis of variance representing the significant parameters in the model is provided in Table 3 and Table 4 shows predicted LW scores and standard errors using the simpler 'three locus' model based on the 2010 and 2011 data. The models for the 2010 and 2011 LW data explained 64 and 66 % of the phenotypic variation. The model for 2010 was simpler and only required inclusion of parameter estimates for additive effects of uniparental marker loci on chromosomes 2, 9, and 10, as well as the interaction between the loci on 2 and 9. The model for 2011 is more complex, requiring inclusion of the uniparental loci on 2 and 10, biparental loci on chromosomes 1 and 3, as well as significant interactions between the alleles on chromosomes 2 and 3. Most noticeable are the increased positive and negative effects of the LG2 and LG10 loci on LW in 2011, in comparison with 2010 parameters. It is also striking that the interactions between the chromosome 2 and 3 alleles are having a significant and quite large negative effect on LW values in 2011, somewhat offsetting the increased positive effect of the chromosome 2 additive effect. To understand the effect of the LG9 QTL linked SNP (c2_3066) from 2010 data, the model for 2011 was fitted using the LG9 marker but the effect due to this SNP was non-significant in 2011 effectively giving the same model as before. Thus, we conclude that tuber shape is a highly complex trait in the 06H1 cross and is not adequately explained by a simple two locus model. This observation goes some way to explaining the lower correlation between tuber shape and eye depth in this cross, as compared with previous studies reporting a simpler trait architecture. This paper highlights the contribution of other minor loci contributing towards tuber shape and the interaction effect of some of the minor loci which influence the length and width response effect of the major QTLs identified. The work reported here also highlights the possibility of using early developmental stages as a possible screen for tuber shape in breeding and also in better understanding the biological systems involved during tuber shape development.

Author contributions Conceived and designed the experiments: VY, GJB, CH, SKS, AP. Performed the experiments: CH, VY, KM, MFBD. Analysed the data: AP, VY, KM, CH, SKS, GJB. Wrote the paper: GJB, AP, VY, CH, SKS.

Acknowledgments We gratefully acknowledge the financial support of the The Scottish Government and Mylnefield Research Services. We also acknowledge the assistance of the potato field trialling team at The James Hutton Institute. We thank Julie Graham and Joanne Russell for critical comments on the manuscript.

Conflict of interest The authors declare they have no conflicts of interest.

References

Bonierbale MW, Plaisted RL, Tanksley SD (1988) RFLP maps based on a common set of clones reveal modes of chromosomal evolution in potato and tomato. Genetics 120:1095–1103

Bradshaw JE, Hackett CA, Lowe R, McLean K, Stewart HE, Tierney I, Vilaro MDR, Bryan GJ (2006) Detection of a quantitative trait locus for both foliage and tuber resistance to late blight *Phytophthora infestans* (Mont.) de Bary on chromosome 4 of a dihaploid potato clone (*Solanum tuberosum* subsp *tuberosum*). Theor Appl Genet 113:943–951

Bryan G, McLean K, Bradshaw J, De Jong W, Phillips M, Castelli L, Waugh R (2002) Mapping QTLs for resistance to the cyst nematode *Globodera pallida* derived from the wild potato species *Solanum vernei*. Theor Appl Genet 105:68–77

Felcher KJ, Coombs JJ, Massa AN, Hansey CN, Hamilton JP, Veilleux RE, Buell CR, Douches DS (2012) Integration of two diploid potato linkage maps with the potato genome sequence. PLoS ONE 7:e36347

Graham J, Hackett CA, Smith K, Woodhead M, MacKenzie K, Tierney I, Cooke D, Bayer M, Jennings N (2011) Towards an understanding of the nature of resistance to *Phytophthora* root rot in red raspberry. Theor Appl Genet 123:585–601

Hackett CA, McLean K, Bryan GJ (2013) Linkage analysis and QTL mapping using SNP dosage data in a tetraploid potato mapping population. PloS One 8. doi:10.1371/journal.pone.0063939

Hamilton JP, Hansey CN, Whitty BR, Stoffel K, Massa AN, Van Deynze A, De Jong WS, Douches DS, Buell CR (2011) Single nucleotide polymorphism discovery in elite North American potato germplasm. BMC Genom 12:302

Kloosterman B, Abelenda JA, Carretero Gomez MdM, Oortwijn M, de Boer JM, Kowitwanich K, Horvath BM, van Eck HJ, Smaczniak C, Prat S, Visser RGF, Bachem CWB (2013) Naturally occurring allele diversity allows potato cultivation in northern latitudes. Nature 495:246–250

Li XQ, De Jong H, De Jong DM, De Jong WS (2005) Inheritance and genetic mapping of tuber eye depth in cultivated diploid potatoes. Theor Appl Genet 110:1068–1073

Luo ZW, Hackett CA, Bradshaw JE, McNicol JW, Milbourne D (2001) Construction of a genetic linkage map in tetraploid species using molecular markers. Genetics 157:1369–1385

Maris B (1966) The modifiability of characters important in potato breeding. Euphytica 15:18–31

Potato Genome Sequencing Consortium (2011) Genome sequence and analysis of the tuber crop potato. Nature 475:189–197

Rezvoy C, Charif D, Gueguen L, Marais GAB (2007) MareyMap: an R-based tool with graphical interface for estimating recombination rates. Bioinformatics 23:2188–2189

Sharma SK, Bolser D, de Boer J, Sonderkaer M, Amoros W, Carboni MF, D'Ambrosio JM, de la Cruz G, Di Genova A, Douches DS, Eguiluz M, Guo X, Guzman F, Hackett CA, Hamilton JP, Li G, Li Y, Lozano R, Maass A, Marshall D, Martinez D, McLean K, Mejia N, Milne L, Munive S, Nagy I, Ponce O, Ramirez M, Simon R, Thomson SJ, Torres Y, Waugh R, Zhang Z, Huang S, Visser RGF, Bachem CWB, Sagredo B, Feingold SE, Orjeda G, Veilleux RE, Bonierbale M, Jacobs JME, Milbourne D, Martin DMA, Bryan GJ (2013) Construction of reference chromosome-scale pseudomolecules for potato: integrating the potato genome with genetic and physical maps. G3-genes genomes. Genetics 3:2031–2047

Sliwka J, Wasilewicz-Flis I, Jakuczun H, Gebhardt C (2008) Tagging quantitative trait loci for dormancy, tuber shape, regularity of tuber shape, eye depth and flesh colour in diploid potato originated from six Solanum species. Plant Breeding 127:49–55

Uitdewilligen JGAML, Wolters A-MA, D'Hoop BB, Borm TJA, Visser RGF, van Eck HJ (2013) A next-generation sequencing method for genotyping-by-sequencing of highly heterozygous autotetraploid potato. PLoS ONE 8(5):e62355

van Eck HJ (2007) Genetics of morphological and tuber traits. In: Vreugdenhil D (ed) Potato biology and biotechnology: advances and perspectives. Elsevier, Amsterdam, pp 91–115

van Eck HJ, Jacobs JME, Stam P, Ton J, Stiekema WJ, Jacobsen E (1994) Multiple alleles for tuber shape in diploid potato detected by qualitative and quantitative genetic analysis using RFLPs. Genetics 137:303

Van Ooijen JW (2006) JoinMap 4, Software for the calculation of genetic linkage maps in experimental populations. Kyazma BV, Wageningen, Netherlands

Van Ooijen JW (2009) MapQTL 6, Software for the mapping of quantitative trait loci in experimental populations of diploid species. Kyazma BV, Wageningen, Netherlands

van Os H, Andrzejewski S, Bakker E, Barrena I, Bryan GJ, Caromel B, Ghareeb B, Isidore E, de Jong W, van Koert P, Lefebvre V, Milbourne D, Ritter E, van der Voort J, Rousselle-Bourgeois F, van Vliet J, Waugh R, Visser RGF, Bakker J, van Eck HJ (2006) Construction of a 10,000-marker ultradense genetic recombination map of potato: providing a framework for accelerated gene isolation and a genomewide physical map. Genetics 173:1075–1087

Zeng ZB (1994) Precision mapping of quantitative trait loci. Genetics 136:1457–1468